JOURNAL OF CATALYSIS 10, 153–165 (1968)

Studies on Pore Systems in Catalysts

XI. Pore Distribution Calculations from the Adsorption Branch of a Nitrogen Adsorption Isotherm in the Case of "Ink-Bottle" Type Pores

J. C. P. BROEKHOFF AND J. H. DE BOER

From the Department of Chemical Technology, Technological University of Delft, The Netherlands

Received October 11, 1967

The method of analysis of the adsorption branch of a nitrogen sorption isotherm, as given in Part IX and Part X of this series, is extended to the model of spheroidal cavities. The results of the cumulative calculations are shown to be satisfactory in appropriate cases, provided the necessary corrections for the influence of adsorption are made to the fundamental equations governing adsorption and capillary condensation in spheroidal cavities.

1. Introduction

It has been shown in Parts IX and X of this series (*1*, *2*), that pore distributions may be calculated from the adsorption branch of A-type nitrogen adsorption isotherms, if the model of open cylindrical pores is adopted. Now the model of open cylinders has to be considered as an idealization of reality at best, and A-type hysteresis loops may be found in cases where the characteristic pore shape deviates considerably from the model of ideal cylinders open at both ends. On the other hand, ideal A-type hysteresis loops are encountered quite rarely in practice, and in many cases the hysteresis loop has some E-type characteristics as well. The E-type hysteresis loop has frequently been interpreted as being connected with the existence of ink-bottle type pores, viz., pores consisting of wide bodies fitted with narrow necks.

It has been recognized for many years and even ages, that the presence of ink-bottle type cavities filled with liquid constitutes a special problem in capillarity. Already in 1718, Jurin (*3*) supposed that the emptying of capillary vessels consisting of a wide body with a very narrow neck, for example, a glass bell fitted with a narrow neck, was governed by the dimensions of the capillary neck rather than by the dimensions of the bell itself. Here we are dealing with a sort of macroscopic "ink-bottle." In more recent times, it was Kraemer (*4*) who suggested that in porous systems pores of the ink-bottle type might occur, and that capillary condensation during adsorption in such pores is governed by the radius of curvature of the wide body of the pores, whereas upon desorption the narrow neck is the factor determining the emptying of the pores. This point of view has been worked out by McBain (*5*) and by Cohan (*6*) as one of the possible explanations for the existence of sorption hysteresis in porous adsorbents. Although this point of view seems to have been accepted by most of the workers in the field, only a few instances are known where the ink-bottle model has been applied to the calculation of pore distributions from nitrogen sorption isotherms. De Boer *et al.* (*7*) have shown that in the case of ink-bottle type pores the adsorption branch may be used successfully in the calculation of pore-size distributions.

2. Two Types of Ink Bottles

In the following discussion we will denote by an ink-bottle pore a pore with a

wide body and a narrow neck. Whether such a pore gives rise to an A-type hysteresis loop or rather to an E-type hysteresis loop depends on the relative magnitude of the radii of curvature of the wide parts and of the narrow necks of the pore, as was shown before by de Boer (*8*). Schematically, another distinction may be made and will prove useful in the thermodynamic discussion that will be given in the next section. In extreme cases the wide body of the pore may exhibit two equal radii of curvature, viz. spheroidal cavities, or may exhibit only one finite radius of curvature, viz. cylindrical tubes. Although the real shape of the ink-bottle capillary may be somewhere in between these extremes, such a distinction is essential in discussing the behavior on filling of the pore during adsorption.

Type I Ink Bottles

By Type I ink bottles we shall denote spheroidal cavities fitted with a narrow neck, which may be considered to be either cylindrical or slit-shaped. During adsorption at some time of the adsorption process this neck will be blocked with capillary condensate, without essentially blocking the transport of molecules from the surrounding gas phase to the inner parts of the pores, as diffusion of adsorbed molecules may take place from the capillary condensate in the necks. The adsorbed layer is concavely curved with two equal radii of curvature and upon increase of pressure this adsorbed layer grows until a critical thickness t_{cr} has been reached, leading to a sudden filling of the whole body of the pore with capillary condensate. Here the stability of the doubly curved meniscus determines the behavior upon adsorption, just as in the case of the singly curved meniscus with open cylindrical pores, discussed in the preceding parts of this series.

Upon desorption the evaporation from the body of the pore is determined by the dimensions of the neck of the pore. Pores exhibiting this behavior will be found among the shape groups II-b and XV according to the classification of de Boer (*8*), whereas, possibly, pores belonging to shape group XIV, will show the same behavior. As the shape group XV is found in cases where the porous material is constituted of small particles packed together, this type of behavior will be encountered quite frequently in practice. This type of ink bottles is schematically represented in the right-hand part of Fig. 1.

Type II Ink Bottles

As was stated before, Type II ink bottles may be visualized to consist of long cylindrical tubes fitted with a narrow neck at one end, whereas the other end may be closed, or consist of another narrow neck. The moment the neck is filled with capillary condensate during adsorption, inside the cylinder there is a meniscus formed at both ends of the cylinder. This meniscus is essentially the same meniscus as the one present in a cylindrical pore, closed at one end, during desorption. As will be shown in

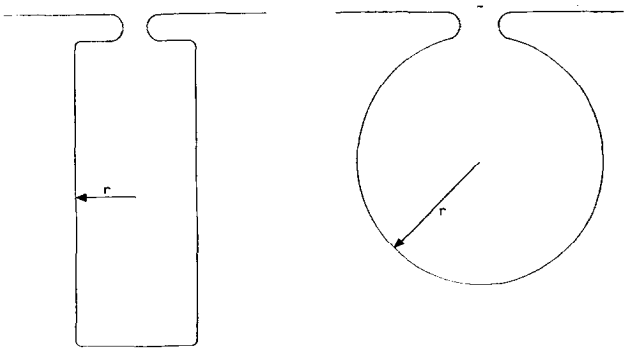

FIG. 1. *Right:* Type I ink bottle, wide part of the pore is essentially spheroidal in shape. *Left:* Type II ink bottle, wide part of the pore is essentially cylindrical in shape.

Part XII of this series, such a meniscus in general has, at each point of the meniscus, two different radii of curvature, as a consequence of the influence of the walls of the pore on the thermodynamic properties of the capillary condensed liquid. At low pressure such a meniscus is stable only at the ends of the pores. As soon as the pressure has reached p_D, the pressure whereupon capillary desorption has been calculated to take place in cylindrical pores according to Part IX of this series [Eq. (16)], this meniscus is stable at every position in the cylindrical part of the pores. Upon increase of pressure above p_D the meniscus vanishes by complete filling of the pore by capillary condensate. We may conclude that the adsorption branch of a Type II ink bottle should coincide with the desorption branch of an isotherm measured on ideal open cylinders with the same radius. If no narrow neck were present but only a closing of the cylinder at one end, then the adsorption branch and the desorption branch would completely coincide and no hysteresis will be observed at all. This is the model of ideal cylinders closed at one end.

In Type II ink bottles again the narrow neck causes a delay in the evaporation upon desorption and hysteresis will be observed. The discussion of the behavior upon adsorption of this type of ink bottles has to be postponed to Part XII of this series, where the shape of the meniscus present in a cylindrical pore during desorption will be discussed in more detail.

Ink bottles exhibiting Type II behavior may be found among the shape groups II-a, IV, VI, and VII of the classification of de Boer (*8*). This type of ink bottle is schematically represented in the left hand side of Fig. 1. In the present article we will restrict ourselves to Type I ink bottles.

3. Thermodynamic Treatment of the Filling of Type I Ink Bottles

A. The Adsorption Branch

The thermodynamic treatment of the filling of ink-bottle pores of Type I is exactly analogous to that given for open cylindrical pores given in Part IX of this series (*1*).

Consider a spheroidal cavity with radius r, carrying an adsorbed layer of thickness t_a at its walls. Upon transferring dN moles of gas to the adsorbed layer at constant temperature and pressure, the free enthalpy of the system (pore + adsorbed layer + gas phase) is changed by

$$dG_{p,T} = (\mu_c - \mu_g)\, dN + \gamma\, dA \qquad (1)$$

where μ_c and μ_g are the thermodynamic potentials of the adsorbed phase and the gas phase, respectively, γ is the surface tension, and dA is the change in free surface area of the adsorbed film upon addition of dN moles to it.

Clearly for a spheroidal cavity, dA is related to dN by

$$dA/dN = -2V_m/(r - t_a) \qquad (2)$$

where V_m is the molar volume of the adsorbate, in the present discussion, as a first approximation, again taken to be equal to that of the bulk liquid at the same temperature.

Insertion of (2) into (1) results in

$$dG/dN_{p,T} = \mu_c - \mu_g - 2\gamma V_m/(r - t_a) \qquad (3)$$

In the usual treatment of capillary condensation it is customary to take μ_c to be constant and equal to that of the bulk liquid, in which case μ_c and μ_g may be related to the saturation pressure of the bulk liquid p_0 by $\mu_c - \mu_g = RT \ln(p_0/p)$.

In that case Eq. (3) could be written as

$$dG/dN_{p,T} = RT \ln(p_0/p) - 2\gamma V_m/(r - t_a) \qquad (4)$$

In equilibrium, $dG/dN_{p,T} = 0$, and for the vapor pressure of an adsorbed film of thickness t_a, the resulting equation would be

$$RT \ln(p_0/p) = 2\gamma V_m/(r - t_a) \qquad (5)$$

This relation would be the analog for spheroidal cavities of Cohan's equation for open cylindrical pores. It is, however, easy to show that at *no* thickness t_a the adsorbed film would be stable, if it obeyed (5). For, as a necessary condition of stability

$$d^2G/dN^2_{p,T} \geq 0 \quad (6)$$

Differentiating (4) at constant p and T yields the expression

$$d^2G/dN^2_{p,T} = [-2\gamma V_m/(r - t_a)^2]\, dt/dN \quad (7)$$

which is negative for every value of t_a and so (6) is never satisfied. It must, consequently, be concluded that (5) has no physical significance and may not be applied to the calculation of pore distributions. The reason for this is that the assumption of μ_c as constant and equal to μ_L, the thermodynamic potential of the bulk liquid, is erroneous. As was explained in Part IX of this series, μ_c is dependent on the distance to the pore wall and thus on t_a. It is advantageous to express the difference between μ_c an μ_L by a relation of the type

$$\mu_c = \mu_L - F(t) \quad (8)$$

where $F(t)$ is an empirical function, which under certain simplifying assumptions may be derived from the universal t curve of multimolecular adsorption.

Introducing (8) into (3) results in the following relation:

$$dG/dN_{p,T} = RT \ln(p_0/p) - F(t) - 2\gamma V_m/(r - t) \quad (9)$$

In equilibrium, $dG/dN_{p,T} = 0$, and for the equilibrium vapor pressure and thickness t_e of the adsorbed layer the following equation results:

$$RT \ln(p_0/p) - F(t_e) = 2\gamma V_m/(r - t_e) \quad (10)$$

From (10), at each pressure, the thickness of the adsorbed layer corresponding to a pore radius r may be calculated if $F(t)$ is known. As a consequence, the thickness of the adsorbed layer at a certain given pressure is different for each radius of the pore. The next question is, whether the thickness t_e calculated from (10), corresponds with a stable equilibrium. To solve this question (9) is differentiated at constant p and T, resulting in

$$d^2G/dN^2_{p,T} = [-dF(t)/dt - 2\gamma V_m/(r - t)^2]\, dt/dn \quad (11)$$

According to (6), a sufficient requirement for stability is

$$-dF(t)/dt - 2\gamma V_m/(r - t)^2 \geq 0 \text{ for } t = t_e$$

It follows immediately that there must be a critical thickness t_{cr}, given by

$$-dF(t)/dt - 2\gamma V_m/(r - t)^2 = 0 \text{ for } t = t_{cr} \quad (12)$$

Thus, for each pore radius, a corresponding value of t_{cr} may be calculated. Whenever for a certain pore radius and pressure, t_e as calculated from (10) exceeds t_{cr} as calculated from (12), the adsorbed layer is no longer stable and complete filling of the pore occurs. It must be realized, however, that already for values of t_e below t_{cr} the equilibrium is only metastable with respect to complete filling of the pore, just as was the case for cylindrical pores open at both ends. This will be shown in the next part of this section.

B. Total Change in Free Enthalpy upon Complete Filling

The question arises whether, thermodynamically, the adsorption branch in the case of Type I ink bottles is a stable or only a metastable branch. In order to investigate this question on theoretical grounds, Eq. (3) may be integrated at constant p and T with respect to t, taking as the lower bound t_a, of Section 3A, the upper bound t_r being smaller or equal to r

$$\Delta G_{p,T} = \int_{N_a}^{N_r} \mu_c - \mu_g - \frac{2\gamma V_m}{(r - t)}\, dN$$

$$= \int_{t_a}^{t_r} \frac{4\pi(r - t)^2}{V_m}\left[\mu_c - \mu_g - \frac{2\gamma V_m}{(r - t)}\right] dt \quad (13)$$

If t_r is taken to be equal to r, this equation represents the total change in free enthalpy upon complete filling of the pore. If in (13) μ_c is taken to be equal to μ_L, the classical point of view, the following relation results:

$$\Delta G_{p,T} = \frac{4\pi(r - t_a)^3}{3V_m} RT \ln\left(\frac{p_0}{p}\right) - 4\pi(r - t_a)^2\gamma \quad (14)$$

Capillary condensation may take place without a change in free enthalpy of the system, whenever $\Delta G_{p,T} = 0$,

$$RT \ln(p_0/p_D) = 3\gamma V_m/(r - t_a) \quad (15)$$

where p_0 is the equilibrium pressure, where emptying *should* occur if no retardation phenomena prevented it. If we make a plot

of (14), that is of ΔG against t at constant p and T, then the resulting lines are exactly analogous to that of Fig. 1 of Part IX of this series. This means that although filling at the pressure p_D of (15) would correspond to a thermodynamically stable situation, filling does not occur on account of the existence of a free enthalpy barrier separating t_a and r.

This barrier is seen to vanish as soon as $d(\Delta G)/dt = 0$ for $t = t_a$, resulting in Eq. (5). Again, the value t_a does not correspond to a minimum in the free enthalpy of the system and thus not to an equilibrium thickness of the adsorbed layer. In order to remove this difficulty it is necessary to introduce (8) into (13), resulting in

$$\Delta G_{p,T} = \int_{t_e}^{t_r} \frac{4\pi(r-t)^2}{V_m} \times \left[RT \ln\left(\frac{p_0}{p}\right) - F(t) \right] dt - 4\pi(r-t_e)^2\gamma \tag{16}$$

Again taking for the upper bound of integration r and putting $\Delta G_{p,T}$ equal to zero, we find for the equilibrium pressure of filling p_D

$$r - t_e = \frac{3\gamma V_m}{RT \ln(p_0/p_D)} + \frac{\int_{te}^{r}[3(r-t)^2F(t)]\,dt}{(r-t_e)^2RT \ln(p_0/p_D)} \tag{17}$$

where t_e is given by (10). That filling does not occur at the pressure p_D of (17), has to be attributed to the existence of a potential barrier between t_e and r. This barrier vanishes as soon as t_e has reached t_{cr}, viz. for $d(\Delta G)/dt = 0$ for $t = t_e$. The corresponding value of t_e is the solution of (12). The situation is exactly analoguous to that of Fig. 2 of Part IX. For each value of r, a value of t_e corresponding to p_D may be calculated. For every value of t_e between this value and t_{cr}, the adsorbed layer is metastable with respect to the situation where the pore is completely filled with capillary condensate. Thus, part of the adsorption branch is thermodynamically metastable.

Upon desorption, emptying of pores would be expected for pressures lower than p_D of Eq. (17), while Eq. (15) holds in the classical point of view. As there is no means of establishing an equilibrium path of desorption in the case of spheroidal cavities, desorption is determined by the radius of the narrow necks of the cavities and desorption is no equilibrium process as regards the emptying of the cavities.

It may be noteworthy that Eq. (15) and (17), apart from the factor 3 instead of 2, are relations of the Kelvin-type, indicating the pressure at which emptying of the pore would be thermodynamically possible. These equations may not be obtained by application of the classical Kelvin formula to the desorption situation as no radius of curvature may be given for the desorption situation. The present method has the advantage that relations of the Kelvin type may be obtained without introduction of the actual adsorption or desorption mechanism, in accordance with the thermodynamic character of the derivation.

The foregoing equations strictly apply only to Type I ink bottles. For Type II ink bottles the adsorption branch corresponds to the desorption branch of open cylinders and thus the whole adsorption branch corresponds to stable states. In both cases the adsorption branch may be described by means of thermodynamic equilibrium conditions, whereas the desorption branch may not be described in such a way and thus does not lend itself to the calculation of pore distributions. It is to be noted that although pores of shape groups belonging to either Type I or Type II ink-bottle pores may occur quite frequently in porous materials, it is a common practice to use the desorption branch of the isotherm for the calculation of pore distributions. In the cases of pores with an ink-bottle shape, this procedure may not be justified.

4. Numerical Evaluation of the Equations Governing the Adsorption of Nitrogen in Type I Ink-bottle Pores

Making use of the empirically found representations for the adsorption of nitrogen at its normal boiling point at noncurved surfaces of inorganic oxides and similarly behaving substances as graphitized carbon blacks and barium sulfate, as given in Part

TABLE 1

THE EQUILIBRIUM THICKNESS, (t_e), OF THE ADSORBED LAYER (Å) IN SPHEROIDAL CAVITIES AS A FUNCTION OF r AND p/p_0

p/p_0	r(Å) =									
	∞	151.5	78.14	51.46	38.24	30.09	24.23	19.92	16.20	12.61
0.9	14.92	29.61								
0.8	10.57	12.07	17.26							
0.7	8.57	9.34	10.50	14.23						
0.6	7.36	7.83	8.39	9.36	12.16					
0.5	6.50	6.75	7.09	7.59	8.37	10.39				
0.4	5.71	5.88	6.10	6.39	6.79	7.43	9.35			
0.3	5.01	5.14	5.28	5.46	5.69	6.00	6.53	8.04		
0.2	4.36	4.45	4.54	4.65	4.78	4.95	5.18	5.57	6.80	
0.1	3.68	3.73	3.78	3.84	3.91	3.99	4.10	4.25	4.51	5.17

X of this series (*2*), we may write for (8), the relation governing the thickness of the adsorbed layer in a spheroidal cavity as a function of relative pressure and pore radius

$$\log(p_0/p) - 13.99/t_e^2 + 0.034 = 4.05/(r - t_e) \text{ for } t_e \leq 10 \text{ Å} \quad (18a)$$

$$\log(p_0/p) - 16.11/t_e^2 + 0.1682 \exp(-0.1137 t_e) = 4.05/(r - t_e) \text{ for } t_e > 10 \text{ Å} \quad (18b)$$

For each value of the pore radius r and for each relative pressure, (18a) or (18b) may be solved for t_e, most conveniently by means of iteration methods, e.g., the Newton-Raphson method.

An abbreviated table of t_e as a function of r and p/p_0 for nitrogen sorption at its normal boiling point is reproduced in Table 1.

Just as was done in the preceding part of this series, again we may define a formal thickness t_f as

$$t_f = V_a/S \quad (19)$$

V_a representing the volume adsorbed in a certain pore of radius r, and S the corresponding surface area. For a spheroidal pore, t_f is obviously related to t_e by

$$t_f = t_e - (t_e^2/r) + (t_e^3/3r^2) \quad (20)$$

In Table 2 the formal thicknesses t_f corresponding to t_e of Table 1 are gathered. Table 2 indicates that, although the equilibrium thickness of the adsorbed layer is considerably larger than that corresponding to the thickness on a noncurved surface at the same pressure, the formal thickness in most of the cases is of the same magnitude and even somewhat less than that on a

TABLE 2

THE FORMAL THICKNESS, (t_f), OF THE ADSORBED LAYER (IN Å) IN SPHEROIDAL CAVITIES AS A FUNCTION OF r AND p/p_0

p/p_0	r(Å) =									
	∞	151.5	78.14	51.46	38.24	30.09	24.23	19.92	16.20	12.61
0.9	14.92	24.20								
0.8	10.57	11.14	13.73							
0.7	8.57	8.78	9.15	10.66						
0.6	7.41	7.43	7.53	7.76	8.70					
0.5	6.50	6.45	6.47	6.53	6.67	7.21				
0.4	5.71	5.66	5.64	5.63	5.66	5.75	6.21			
0.3	5.01	4.97	4.93	4.90	4.88	4.88	4.93	5.23		
0.2	4.36	4.32	4.28	4.24	4.21	4.18	4.15	4.16	4.35	
0.1	3.68	3.64	3.61	3.56	3.52	3.48	3.44	3.41	3.37	3.44

noncurved surface. This means that a t plot of the adsorption isotherm in the case of Type I ink bottles will show no deviations from the linear plot or at most a downward deviation, as long as no actual capillary condensation leading to complete filling of the cavity takes place. If for the narrowest group of pores present t_e has reached t_{cr}, an upward deviation indicates the onset of capillary condensation. This important result indicates that a pore distribution has to be extended from saturation down to the pressure where the first upward deviation from the linear t plot occurs.

For each pore radius, t_{cr} may be calculated from the equations

$$27.98/t_{cr}^3 = 4.05/(r - t_{cr})^2 \text{ for } t_{cr} \leq 10 \text{ Å} \quad (21a)$$

$$32.22/t_{cr}^3 - 0.1682 \times 0.1137 \exp(-0.1137 t_{cr}) = 4.05/(r - t_{cr})^2 \text{ for } t_{cr} > 10 \text{ Å} \quad (21b)$$

These equations immediately follow from (12) and the empirical representations of the t curve as given in the preceding part of this series. They may be solved by means of the iteration methods mentioned before. The results of the solution of (21) may be combined with (18), yielding the pressure at which a spheroidal cavity with specified radius completely fills with capillary condensate. In Table 3 the radius corresponding to a number of relative pressures, as calculated from (18) and (21), is represented.

For the sake of comparison we include in Table 3 the radii corresponding to the same relative pressures, as calculated by means of (5), viz. the radii that would follow from the application of the Kelvin equation to the doubly curved adsorbed layer at the walls of the spheroidal cavity, in the same way as Cohan's equation was used for the capillary condensation in open cylinders.

Table 1 and Table 3 contain all the information necessary to perform a pore distribution calculated from the adsorption branch of a nitrogen sorption isotherm in the case of Type I ink bottles. In the next section a general formula will be derived for the calculation of pore distributions

TABLE 3

RADII OF SPHEROIDAL CAVITIES FILLING AT CERTAIN SPECIFIED RELATIVE PRESSURES, CALCULATED WITH THE AID OF EQ. (21), AS COMPARED TO THOSE CALCULATED BY MEANS OF EQ. (5)

p/p_0	r (Å) Eq. (21)	r (Å) Eq. (5)
0.9975	4456	3844
0.9925	1593	1307
0.9875	994.5	792.8
0.9825	731.0	569.8
0.9775	581.6	444.7
0.9725	484.9	364.5
0.9675	416.9	308.9
0.9625	366.4	268.1
0.9575	327.2	237.0
0.9525	295.9	212.4
0.9475	270.2	192.5
0.9425	248.7	176.1
0.9375	230.4	162.3
0.9325	214.6	150.6
0.9275	200.8	140.5
0.9225	188.7	131.6
0.9175	177.9	123.8
0.9125	168.2	117.0
0.9075	159.4	110.8
0.9025	151.1	105.3
0.89	134.6	93.62
0.87	114.0	79.57
0.85	98.87	69.20
0.83	87.27	61.22
0.81	78.14	54.88
0.79	70.76	49.65
0.77	64.69	45.38
0.75	59.58	41.77
0.73	55.22	38.65
0.71	51.46	35.95
0.69	48.17	33.57
0.67	45.26	31.45
0.65	42.67	29.58
0.63	40.35	27.88
0.61	38.24	26.34
0.59	36.33	24.95
0.57	34.58	23.66
0.55	32.96	22.49
0.53	31.47	21.39
0.51	30.09	20.38
0.49	28.40	19.44
0.47	27.28	18.56
0.45	26.21	17.73
0.43	25.20	16.95
0.41	24.23	16.21
0.39	23.30	15.51
0.37	22.41	14.85
0.35	21.55	14.22

TABLE 3 (*Continued*)

p/p_0	r (Å) Eq. (21)	r (Å) Eq. (5)
0.33	20.72	13.61
0.31	19.92	13.03
0.29	19.14	12.47
0.27	18.38	11.93
0.25	17.64	11.41
0.23	16.91	10.90
0.21	16.20	10.40
0.19	15.49	9.91
0.17	14.78	9.43
0.15	14.07	8.95
0.13	13.35	8.47
0.11	12.61	7.97

from the adsorption branch in the case of spheroidal cavities.

5. Derivation of a General Formula for the Calculation of Pore Distributions

For the calculation of pore distributions the adsorption branch is divided into certain specified intervals of relative pressure, these intervals being bound by x_k, the lower relative pressure bound, and $x_{(k-1)}$, the next higher relative pressure bound. Again the calculation is performed in the reverse sequence from the actual adsorption measurement and calculation is started at the highest relative pressure. Lowering the relative pressure from $x_{(k-1)}$ to x_k results in a change in the volume of the condensed phase present in the pores, dV_k^c, consisting of two contributions:

(a) Over the kth interval pores are emptied, the mean pore radius of this group of pores being r_k, the radius corresponding to the mean relative pressure over the kth interval, as taken from Table 3. If the total surface area of this kth group of pores is denoted by S_k, then this part in the change of volume of the condensed phase obviously is equal to

$$(r_k - t_{rk,xk})^2/3r_k^2 \times S_k,$$

$t_{rk,xk}$ being the thickness of the remaining adsorbed layer at the wall of the pores of mean radius r_k at the lowest relative pressure of the kth interval.

(b) For the k-1 groups of pores with radius larger than r_k, already emptied at the relative pressure $x_{(k-1)}$ except for an adsorbed layer, the adsorbed layer in all these pores is diminished in thickness upon decreasing the relative pressure from $x_{(k-1)}$ to x_k. If we denote the surface area present in the ith group of pores, with radius r_i, by S_i, then this part in the change of volume of the condensed phase amounts to

$$\sum_{i=1}^{k-1} \frac{S_i}{3r_i^2}\left[(r_i - t_{ri,xk})^3 - (r_i - t_{ri,x(k-1)})^3\right]$$

Adding these two contributions, equating to dV_k^c and solving for S_k results in the pore distribution formula

$$S_k = \frac{3r_k^2}{(r_k - t_{rk,xk})^3}\left\{dV_k^c - \sum_{i=1}^{k-1} \frac{S_i}{3r_i^2} \times \left[(r_i - t_{ri,xk})^3 - (r_i - t_{ri,x(k-1)})^3\right]\right\} \quad (22)$$

For the actual calculation of pore distributions (22) may be applied, making use of the values of $t_{ri,xk}$ from Table 1 and of the values of S_i from each preceding step of the calculation. The pore volume of each group of pores is related to S_k by

$$S_k = 3V_k/r_k \quad (23)$$

The application of (22) is tedious and lengthy for routine work, as for each step of the calculation the summation series at the right side of (22) has to be calculated again. If a high-speed electronic computer is present, the application of (22) is easy and straightforward and no difficulties are encountered in the practical application. A table of the required value of $t_{ri,xk}$ may be set up once and used every time. The cumulative distribution functions S_{cum} and V_{cum} are obtained by simply adding S_k and V_k obtained from each step down to a relative pressure where the first deviation from the linear t plot occurs.

If we would have neglected the influence of r on the thickness of the adsorbed layer and made use of the values of r of (5), viz. the classical conception of the application of Kelvin's equation to the calculation of pore distributions, then (22) would reduce to a far more simple form

$$S_k = \frac{3r_k^2}{(r_k - t_{xk})^3}\left[dV_k^c - (t_{x(k-1)} - t_{xk}) \times \sum_{i=1}^{k-1} S_i + (t_{x(k-1)}^2 - t_{xk}^2)\sum_{i=1}^{k-1}\frac{S_i}{r_i} - (t_{x(k-1)}^3 - t_{xk}^3)\sum_{i=1}^{k-1}\frac{S_i}{3r_i^2}\right] \quad (24)$$

Equation (24) is analogous to the equation given before by Montarnal (*9*) and by de Vleesschauwer (*10*) for the case of cylindrical pores. Application of (24) is possible even for desk calculations, because of the relatively simple form of the summation series at the right side of (24). As will be shown in the next section, the application of this equation is not only unjustifiable on the theoretical grounds discussed in Section 3, but also leads to most improbable results.

6. Application of the General Equations to the Actual Calculation of Pore Distributions

It is generally supposed than in porous glass, pores of the ink-bottle type are present. Of the rather extensive literature present on the adsorption in porous glass, we choose two isotherms from the series measured by Emmett and Cines (*11*) and calculated the pore-size distribution and the cumulative pore volume and surface area from the adsorption branch of the isotherm. A t-plot of the nitrogen isotherms on the samples of porous glass No. 4 and No. 6 is represented in Fig. 2. The published isotherms of Emmett and Cines were not represented as ml STP per gram but only as ml STP so the surface area calculated from the isotherm is not specific. The t plot of sample No. 4 shows the presence of micropores. The total surface area equals 38.6 m², whereas the presence of a second straight portion indicates the presence of wider pores with a surface area of 25.1 m². The first deviation from this second straight part occurs at a relative pressure of 0.37 and the pore distribution calculation has been extended down to that relative pressure. The cumulative surface area should be compared to this last value, as there is no sense in calculating the distribution of micropores by means of the concept of capillary condensation, the dimension of these pores being definitely too small for the concept of a liquid meniscus. A t plot of the sample porous glass No. 6 of Emmett and Cines shows no indication of the presence of micropores. The total surface area as calculated from a straight line through the origin, is equal to 20.6 m². The first deviation from the straight part of the t plot occurs at $p/p_0 = 0.44$. Here we should find the total surface area on applying (22) down to a relative pressure of 0.44. The samples of Part X all showed

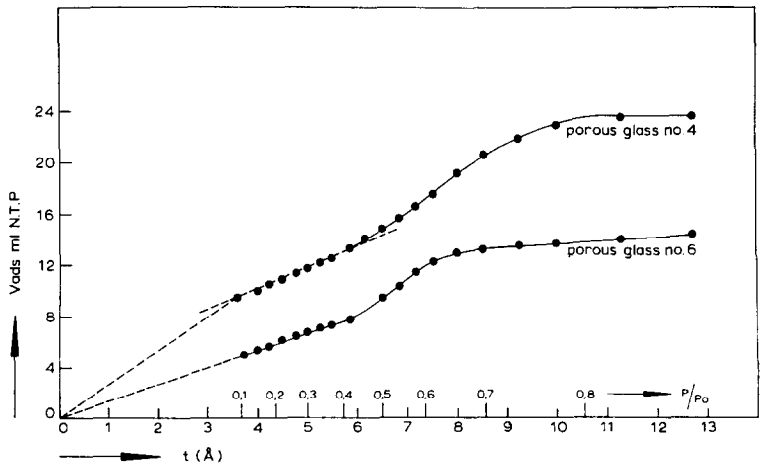

FIG. 2. t plot of the nitrogen isotherms of the samples porous glass No. 4 and porous glass No. 6 as measured by Emmett and Cines.

TABLE 4

CUMULATIVE SURFACE AREAS AND PORE VOLUMES FOR THE MODEL OF SPHEROIDAL CAVITIES, AS CALCULATED BY MEANS OF EQ. (22), AS COMPARED TO THE RESULTS OF A CLASSICAL PORE DISTRIBUTION CALCULATION ALONG THE ADSORPTION BRANCH

Sample code	p/p_0, first deviation from t plot	p/p_0, closing point of hysteresis loop	S_{BET} (m^2/g)	S_{cum} (m^2/g)	$S_{cum,class}$ (m^2/g)	V_p (ml/g)	V_{cum} (ml/g)	$V_{cum,class}$ (ml/g)
Porous glass no. 4[a]	0.38	0.42	25.1[d]	21.1	37.5	0.0305	0.0287	0.0335
Porous glass no. 6[a]	0.44	0.50	20.6[d]	17.3	31.4	0.0227	0.0205	0.0242
By 580[b]	0.24	0.42	243	245	513	0.434	0.425	0.488
By 750[b]	0.24	0.46	134	150	241	0.464	0.472	0.502
A 120[b]	0.26	0.40	609	679	1034	2.03	2.05	2.18
A 270[b]	0.30	0.51	556	600	967	1.74	1.77	1.92
A 450[b]	0.34	0.54	414	525	853	1.78	1.84	1.99
A 750[b]	0.63	0.63	280	285	464	2.05	2.02	2.19
MiBo 5[b]	0.26	0.38	255	278	449	0.496	0.505	0.556
BoW 450[b]	0.40	0.70	68[d]	63	97	0.479	0.477	0.500
ZrO_2 280[c]	0.14	0.42	240	266	519	0.252	0.254	0.314
ZrO_2 320[c]	0.19	0.45	180	203	392	0.201	0.204	0.253
ZrO_2 390[c]	0.36	0.53	100	107	192	0.183	0.186	0.218
ZrO_2 450[c]	0.64	0.64	64	64	107	0.190	0.191	0.213

[a] P. H. Emmett and M. Cines, ref. (*11*).

[b] Isotherms measured by Lippens, refs. (*12*) and (*13*).

[c] Isotherms measured by Rijnten, refs. (*14*) and (*15*).

[d] Surface areas determined from the slope of the linear part of the t plot.

a more or less pronounced A-type adsorption isotherm. As de Boer (*8*) has shown, pores belonging to the shape groups II-b and the like, exhibit A-type hysteresis loops, although according to the classification of the present paper they definitely belong to the Type I ink-bottle class. Consequently, the model of spheroidal cavities is also a possibility for those isotherms, and the pore distribution has been recalculated for all those isotherms.

The results are gathered in Table 4. For the sake of comparison, the calculations have been repeated, making use of the solutions of (5) and the pore distribution formula (24). The cumulative results of this latter calculation have been denoted by S_{class} and V_{class}.

7. DISCUSSION

The results presented in Table 4 indicate that in most of the cases under consideration the model of spheroidal cavities is as adequate as the model of open cylindrical pores, provided the corrections discussed in Section 3 are applied to the fundamental formulas for the calculation. In the classical application of Kelvin's equation the radii of either open cylindrical or spheroidal pores filling at a certain relative pressure are relatively so small as to result in improbably high values for the cumulative surface area. Although it might be argued that the model of open cylindrical pores is an unrealistic one, the model of spheroidal cavities should be a reasonable good approximation at least for porous materials built up of small particles packed together. Here the corrected formulas of Section 3 and 4 give satisfactory results at least in a first approximation. On the other hand, in some cases, the results of the cumulative calculations of surface area and pore volume are definitely too high, e.g., for the samples A 120, A 270, and A 450 of the series of nitrogen sorption isotherms measured on aluminum oxide by Lippens. In these cases, it will be shown in the next article of this series that the model of Type II ink bottles is as useful or even more useful than that of open cylindrical pores or Type I ink bottles. In that case the

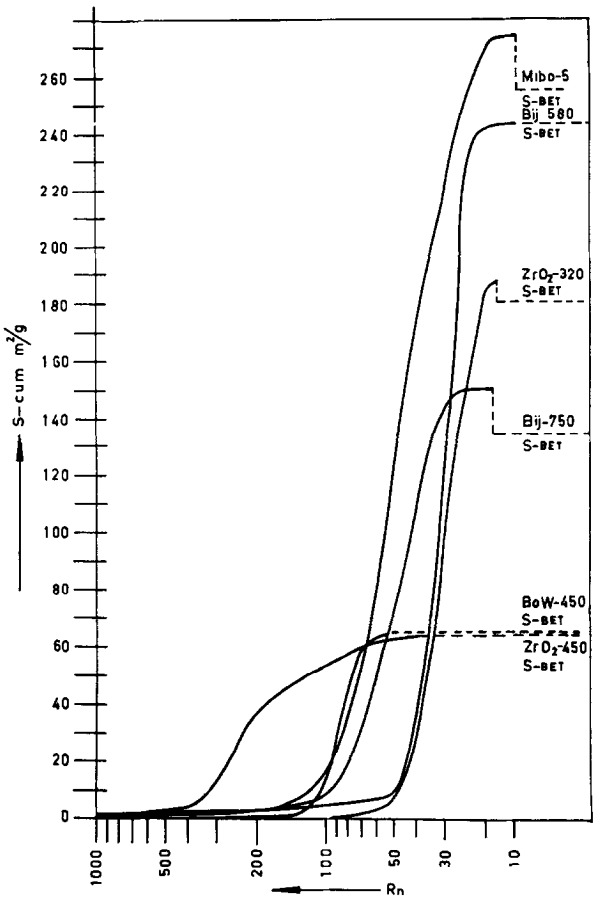

FIG. 3. Examples of pore distribution curves as calculated by means of Eqs. (18) and (21).

adsorption branch has to be calculated with the aid of the radii connected with the desorption from cylindrical pores, which results in a considerable reduction in calculated cumulative surface area. For the other samples a comparison with the results obtained with the aid of the model of open cylindrical pores, indicates that the analysis of the adsorption branch alone is not sufficient to decide between the two alternatives: open cylindrical pores or Type I ink bottles. Here an analysis of the desorption branch is necessary. In the case of open cylindrical pores, it is to be expected that a calculation along the desorption branch with the aid of Eq. (16) of Part IX of this series results in a cumulative surface area comparable to that of the adsorption branch and the BET surface area, whereas in the case of Type I ink bottles no concordance is to be expected from an analysis of the desorption branch, this being a nonequilibrium branch with regard to the spheroidal cavities. In the case of Type II ink bottles an analysis of the desorption branch with the aid of the model of cylindrical pores should lead to too high cumulative results.

Some samples of distribution curves calculated with the aid of the model of spheroidal cavities are given in Fig. 3. For comparision, in Fig. 4 the results of a classical distribution calculation along the adsorption branch, using the same model of spheroidal cavities, are given for the same samples. On the whole, the new method of calculation seems to work satisfactorily in practice. Uncertainties inherent in the present method may be divided into two classes:

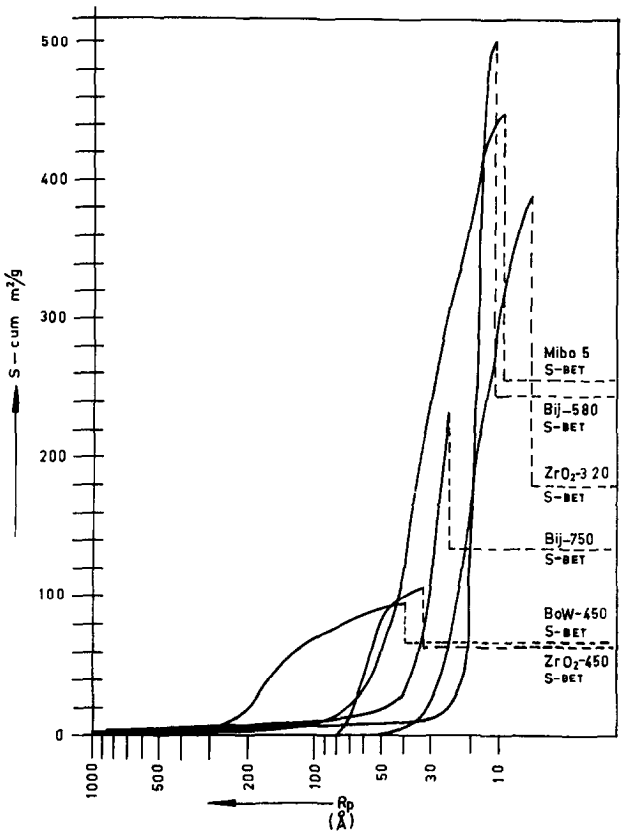

FIG. 4. Examples of pore distribution curves as calculated by means of Eq. (5).

(a) The model of spheroidal cavities even in appropriate cases is an idealization, as the surface of a cavity may not be expected to be spherical even in cases where the pores are present as cavities in between elementary particles of spheroidal shape. Moreover, the pore may have some tubular characteristics as well, or even other shape characteristics.

(b) The simplifying assumptions made in deriving Eq. (10) and (12), which are the same as those discussed in Part IX of this series, viz., constant density of the condensed phase, constant surface tension, and the applicability of classical (macroscopic) thermodynamics to the situation in pores, are certainly not valid for narrow pores, making the applicability of the method to the analysis of the lower part of the adsorption isotherm questionable. At the moment there seems to be no really satisfactory alternative for the analysis of this part of the isotherm in the case of porous substances. It ought to be realized that in such cases also the reliability of the surface area estimation either by means of the BET method or of the t method is questionable.

REFERENCES

1. BROEKHOFF, J. C. P., AND DE BOER, J. H., *J. Catalysis* **9**, 8 (1967) (Part IX).
2. BROEKHOFF, J. C. P., AND DE BOER, J. H., *J. Catalysis* **9**, 15 (1967) (Part IX).
3. JURIN, J., *Phil. Trans.* **30**, 335, 363, 759, 1083 (1718); see *Phil. Trans.* (abridged edition, 1809). **VI**, 355, 739.
4. KRAEMER, E. O., *in* "A Treatise on Physical Chemistry" (H. S. Taylor, ed.), p. 1661. New York, 1931.
5. MCBAIN, J. W., *J. Am. Chem. Soc.* **57**, 699 (1935).
6. COHAN, J. H., *J. Am. Chem. Soc.* **66**, 98 (1944).
7. DE BOER, J. H., LINSEN, B. G., AND HEUVEL, A. v.d., *J. Catalysis* **3**, 268 (1964).

8. DE BOER, J. H., The shape of capillaries, *in* "The Structure and Properties of Porous Materials" (D. H. Everett and F. S. Stone, eds.), Butterworth, London, 1958.

9. MONTARNAL, R., AND CLEMENT, R., *J. Chim. Phys.* **59,** 195 (1962).

10. DE VLEESSCHAUWER, W. F. N. M., PH.D. Thesis, Delft, 1967, p. 122.

11. EMMETT, P. H., AND CINES, M., *J. Phys. Coll. Chem.* **51,** 1260 (1947).

12. LIPPENS, B. C., PH.D. Thesis, Delft, 1961, p. 128.

13. LIPPENS, B. C., AND DE BOER, J. H., *J. Catalysis* **3,** 38 (1964).

14. RIJNTEN, H.TH., PH.D. Thesis, Delft, to be published.

15. DE BOER, J. H., *Proc. Brit. Ceramic Soc.* (No. *5*) p. 5 (1965).